NASA Technical Memorandum 102098

A Model for Prediction of STOVL Ejector Dynamics

Colin K. Drummond
Lewis Research Center
Cleveland, Ohio

Prepared for the
Twentieth Annual Conference on Modeling and Simulation
cosponsored by the University of Pittsburgh, IEEE, and ISA
Pittsburgh, Pennsylvania, May 4–5, 1989

A MODEL FOR PREDICTION OF STOVL EJECTOR DYNAMICS

Colin K. Drummond
National Aeronautics and Space Administration
Lewis Research Center
Cleveland, Ohio 44135

ABSTRACT

A semi-empirical control-volume approach to ejector modeling for transient performance prediction is presented. This new approach is motivated by the need for a predictive real-time ejector sub-system simulation for STOVL integrated flight and propulsion controls design applications. Emphasis is placed on discussion of the approximate characterization of the mixing process central to thrust augmenting ejector operation. The proposed ejector model suggests transient flow predictions are possible with a model based on steady-flow data. A practical test case is presented to illustrate model calibration.

INTRODUCTION

For the short take-off vertical landing (STOVL) aircraft configuration shown in Figure 1, the thrust augmenting ejectors placed at each wing root must be included in the propulsion system simulation. Integrated flight and propulsion control (IFPC) studies require ejector component simulations that must run accurately in "real-time". Since accuracy is typically synonymous with a high level of model detail, constructing a transient ejector model to fit the simulation requirement is not an easy task.

A useful ejector characteristic to know the frequency response of ejector thrust. If the ejector response is outside the bandwidth of the flight control system then a simple quasi-steady ejector model or look-up table is all that is needed. On the other hand, if the ejector response falls within the range of the flight control (or if a new ejector design has an unknown response) a high-fidelity ejector simulation is required; this paper explores an ejector modeling approach to fill the latter requirement.

There are two basic perspectives generally employed to set the mathematical framework for the ejector mass, momentum, and energy balances; the choice is easy when the intended simulation application is considered. One approach is based on first principles and typically blends the full unsteady Navier-Stokes equation with a tubulence model. The result is cast in, for example, finite-difference form. Although this approach provides a desireable ejector *design* flavor to the analysis, the solution to the final set of equations is not amicable to real-time execution in the foreseeable future; another problem concerns identification of the appropriate turbulence model to use for description of the mixing region.

A second, more *analysis* oriented approach, involves a control-volume formulation. Highly detailed descriptions of the mixing region shear layer can be exchanged for a semi-empirical model and the potential to run in real-time. In this paper, the intended ejector application as a force effector leads to tailoring of the semi-empirical model to match thrust predictions (matching is not *primarily* for the field variables). This compromise is acceptable in light of the simplicity the model offers.

An attractive feature of a steady-flow control-volume ejector analysis is the ability to collapse the complex primary and secondary flow mixing process for steady flow into one unknown quantity - the mixing effectiveness parameter β. Although *ideal* mixing yields a mixing parameter of unity, the more typical non-uniform flow profile (non-ideal mixing combined with boundary-layer effects) in real ejector configurations generally produces mixing parameter values between 1.05 and 1.2. The key in a useful control-volume analysis is knowing what the exact mixing effectiveness value is for a given ejector configuration. In the analysis to follow it is assumed steady-state ejector data is available so that β can be backed out.

Under the premise the steady-state ejector model has been "calibrated" (that is, β and all surface integrals are known), the time-dependent *volume*-integrals are the only remaining unknowns to be treated in the control volume analysis of an *unsteady* flow. In the present work, sub-dividing the mixing region (streamwise) into a finite number of subvolumes allows Abramovich-type self-similar turbulent flow profiles to conveniently link the local primary and secondary field variables. The result is a set of equations for each mixing region sub-element containing the desired field variable time derivatives. From this analytic springboard a kinetic energy exchange function is introduced to complete the interaction between the streams and provide closure for the mixing region analysis.

MIXING REGION REPRESENTATION

Numerous finite-volume descriptions for steady-state ejector flows are available in the literature (Drummond[4], Porter and Squires[6], Addy and Dutton[2]). For simplicity in analysis, ejectors are typically divided into inlet, diffuser and mixing regions. Since inlet and diffuser dynamics can, in the first approximation, be assumed away with quasi-steady approximations, only the ejector mixing region shown in Fig. 2 is of interest in the present work. A control-volume mixing region analysis generally involves the one-dimensional mass, momentum and energy equations below:

$$\frac{dm_{cv}}{dt} = -\oint_A \rho \mathbf{v}\cdot\mathbf{n}\,dA \tag{1}$$

$$\frac{d}{dt}\int_V \rho \mathbf{v}\,dV = -\oint_A \rho \mathbf{v}(\mathbf{v}\cdot\mathbf{n})dA - \oint_A \mathbf{n}\cdot(p\mathbf{I})dA \tag{2}$$

$$\frac{d}{dt}\int_V \rho\left(h+\frac{u^2}{2}-\frac{p}{\rho}\right)dV = -\oint_A \rho\left(h+\frac{u^2}{2}\right)\mathbf{v}\cdot\mathbf{n}\,dA \tag{3}$$

These equations reflect the use of the usual assumptions of adiabatic frictionless flow (at the ejector wall) [4]. A steady-flow analysis involves only the surface integrals on the right-hand-side of Eqns.(1)-(4). It is the time derivatives of the volume integrals on the left-hand-side of each equation that characterize the unknown dynamics of the ejector mixing region.

Remark on the Energy Equation

Equation (3) represents the energy equation derived from the first law of thermodynamics -- this form of the energy balance is known as the *general energy equation*. The general energy equation is a balance of energy due to heat and work. The product of the local fluid velocity and the momentum equation (Eqn.2) yields the *mechanical energy equation*. Subtracting the mechanical energy equation from the general energy equation produces the *heat equation*, the latter of which is a simple statement of conservation of heat content in the ejector mixing region,

$$\frac{d}{dt}\int_V \rho\left(h-\frac{p}{\rho}\right)dV \;=\; -\oint_A \rho h\,\mathbf{v}\cdot\mathbf{n}\,dA \qquad (4)$$

It is important to note in the present work that the general energy equation is split into its mechanical and thermal energy components. Although Eqn.(4) is retained to represent the heat balance, a semi-empirical kinetic energy exchange model is substituted for the mechanical energy equation (the details of the function are discussed later). The idea to emphasize here is that an emprically-based transfer function is proposed to be a satisfactory replacement for the detailed mechanical energy modeling that would otherwise be required for the turbulent flow characterization.

Field Variable Approximation

Extensive experimental data supports the basic Abramovich[1] non-dimensional field variable representations of the co-flowing primary and secondary streams. General features of the ejector jet geometric approximation are shown in Fig. 3. Extending from the mixing region inlet plane there exists a *potential-core* region characterized by a fairly uniform centerline velocity, with no transverse component. This is distinguished from the *mixed-flow* region where the centerline velocity decay arises from momentum transport to the entrained fluid. In the characterization of an element of the ejector mixing region, it is assumed the velocity can be approximated by the following 2-D planar turbulent jet self-similar profiles for co-flowing jets:

$$v \;=\; v_e(1-\Phi)+v_m\Phi \;=\; f(\Phi) \qquad (5)$$

where

$$\Phi(\xi) \;=\; \begin{Bmatrix} (1-\xi^{1.5})^2, & 0\le\xi\le 1 \\ 0, & 1\le\xi\le\hat{\xi} \end{Bmatrix} \qquad (6)$$

$$\xi \;=\; x/b, \qquad \hat{\xi} \;=\; B/b \qquad (7)$$

Inclusion of the core region requires a slight modification of these profiles; details are given in Abramovich[1]. Since there is a static pressure matching condition at the jet boundary in the ejector mixing region, a uniform *transverse* pressure distibution must be assumed; in the longitudinal (axial) direction, however, a finite pressure gradient exists -- this feature partially distinguishes free-jet and confined-jet analyses. Although the general ejector model admits a function Λ to characterize the normalized pressure distribution, the uniform transverse pressure suggests

$$\frac{p - p_e}{p_m - p_e} = \Lambda(\xi) = [1, 0 \le \xi \le \hat{\xi}] \tag{8}$$

To reduce confusion in the use of the ideal gas law, pressure and density should have similar profiles,

$$\rho = \rho_e(1 - \Lambda) + \rho_m \Lambda \tag{9}$$

Since these functions imply a uniform temperature profile, a compromise has been introduced in the mixing region representation for temperature; Abramovitch suggests the non-dimensional temperature profile be approximated by the square root of the velocity profile.

Finite Volume Descretization

Figure 4 illustrates the finite volume descretization employed in the present work. Since the implicit assumption has been the self-similar profiles link the primary streams in the transverse direction, descretization occurs only in the streamwise direction. Because the characteristic streamwise velocity is generally "high", very few volumes are needed to capture basic flow effects. Computations in the present work were performed with the mixing region divided into 5 elements.

The combined effect of the analytic interstream relationships and the streamwise descretization is to provide a virtual computational grid, also shown in Fig.4.

Application to the Conservation Equations

Only a summary of the application of the non-dimensional field variable profiles to the control volume conservation equations is presented here since details can be found in reference [4].

Conservation of Mass

For the generic sub-region *k*, bounded by surfaces at *i* and *j*, mass conservation yields

$$\left(\frac{dm}{dt}\right)_k = \dot{m}_i - \dot{m}_j \tag{10}$$

First, the mass flux is written

$$\dot{m}_i = \int_A \rho_i v_i dA = 2W \int_0^{\xi} \rho_i v_i d\xi \tag{11}$$

From which integration over the self-similar profiles yields

$$\dot{m}_i = 2Wb_i\rho_i(0.45v_m + 0.55v_e + (\xi - 1)v_e)_i = 2Wb_iZ_1 \qquad (12)$$

The time-derivative term in the mass conservation equation is given by

$$\left(\frac{dm}{dt}\right)_k = 2WB\Delta z\left(\frac{d\rho}{dt}\right)_j \qquad (13)$$

where the characteristic density for the finite volume is now approximated by the value of the density at station *j* (this is a reasonable assumption as long as field variable gradients are "modest" in size). If the characteristic jet expansion width, *b*, also assumes its value at *j*, then substitution and re-arrangement of the continuity equation yields

$$\left(\frac{d\rho}{dt}\right)_j = \frac{b_iZ_{1,k} - b_jZ_{1,j}}{B\Delta z} \qquad (14)$$

Computation of the jet half-width, *b*, derives from an incompressible flow assumption applied to the *first* finite volume; a rectilinear jet expansion is assumed therefrom and compressible flow restored for subsequent calculations.

Momentum Equation

The procedure described for the continuity equation can be applied to the momentum equation. Omitting the details for brevity, the result for the centerline velocity derivitive is

$$\left(\frac{dv_m}{dt}\right)_j = \frac{\dot{M}_k}{2Wb_j\Delta z} - \frac{v_m + v_eF_1}{\rho}\left(\frac{d\rho}{dt}\right)_j \qquad (15)$$

where

$$F_1 = \frac{\hat{\xi} + 0.45}{0.45} \qquad (16a)$$

$$\dot{M}_k = 2Wb_i\rho_i(Z_{2,i} + \hat{\xi}P_i) - 2Wb_j\rho_j(Z_{2,j} + \hat{\xi}P_j) \qquad (16b)$$

$$Z_{2,i} = \int_0^{\xi}\rho_i v_i^2 d\xi \qquad (16c)$$

Energy Equation

Introduction of an ideal gas assumption simplifies the heat equation to the form

$$\frac{d}{dt}\int pdV = -\oint_A p\gamma\mathbf{v}\cdot\mathbf{n}dA \qquad (17)$$

Non-dimensional velocity and pressure profiles provide the pressure derivative result

$$\left(\frac{dp}{dt}\right)_k = \gamma\frac{b_k Z_1 + b_{k+1} Z_1}{\Delta z B} + (\gamma - 1)\frac{b_k Z_0 - b_{k+1} Z_0}{\Delta z B} \qquad (18)$$

where Z_1 has been derived previously and Z_0 is given at each station by

$$Z_{0,i} = \int_0^{\xi} p_i \Lambda d\xi \qquad (19)$$

Equations (14), (15), and (18) are the three differential equations required for computing the time derivatives of gas density, pressure, and jet centerline velocity in the ejector mixing region. Integration of these equations can be combined with a quasi-steady diffuser analysis to predict the ejector discharge conditions as a function of time. Ejector thrust is approximated by

$$T = \frac{\dot{m} v}{\beta^2} \qquad (20)$$

where β is the mixing effectiveness parameter discussed in the introduction.

Closure of the initial value problem for the mixing region requires an analytic approximation for the mechanical energy removed in the formulation of Eqn.(4). The purpose of the next section is to propose an appropriate function.

Entrained Kinetic Energy Approximation

This section provides an approximation for the turbulent flow kinetic energy exchange mechanism to characterize the influence of primary flow changes on the secondary flow. A discussion of the proposed kinetic energy balance is followed by clarification of the primary and secondary kinetic energy representations.

Kinetic Energy Balance

Computations for a specified steady-state condition show that the change in kinetic energy due to *mixing* is not the same for the secondary flow as it is for the primary. In fact, the gain in kinetic energy of the secondary flow is entirely due to the mixing process, while the mixing loss of the primary flow is only a fraction of its total loss. In balance, however, the total change of kinetic energy of the primary flow is greater than that of the secondary flow.

In the work of Korst and Chow[5] the relationship between the change in entrained flow kinetic energy and the total primary flow kinetic energy for a shear layer is given in functional form by

$$\Delta KE_{1S} = F\left\{KE_{1P}, \frac{\sigma}{z}\right\} \qquad (21)$$

where a reasonable match between theory and experiment is given by

$$\sigma = 12(1 + 0.23 M_{1P}) \qquad (22)$$

The difficulty with the kinetic energy function as given above is that it represents a quasi-steady constant-pressure flow approximation and therefore cannot be used in its present form for the transient flow analysis. To entertain local transport of energy between the primary and secondary flows, consider the change in secondary flow to be a combination of changes in primary and secondary flow kinetic energies due to *mixing alone*,

$$\Delta KE_{1S} = G\left\{\Delta KE_{1P,m}, \Delta KE_{1S,m}, \frac{\sigma}{z}\right\} \tag{23}$$

where the subscript m denotes the change in kinetic energy due exclusively to mixing. In conjunction with numerical experiments, a specific form for the function has been determined to be

$$\Delta KE_{1S}^{t+\Delta t} = \Delta KE_{1S,m}^{t+\Delta t} + \Delta KE_{1P,m}^{t} C_1 \left(\frac{\sigma}{z}\right)^2 \tag{24}$$

Note the introduction of this engineering approximation also results in the introduction of an undetermined constant, C_1. This value is established in the present work by matching transient solution asymptotes with steady-state performance data; an example is presented later a the case study. The alternative is to establish N computations of the kinetic energy exchange to coincide with the N control volumes of the mixing region; the present method is more rapid since it permits post-processing of information at the completion of mixing region calculations.

Knowledge of the total change in secondary flow kinetic energy permits updates to the secondary flow state during integration of the field variable time derivatives. After the velocity of the secondary flow has been extracted from the new secondary flow kinetic energy, the new inlet density and pressure are computed from an ideal flow inlet analysis. Brief descriptions of the mixing kinetic energies are given below.

Secondary Stream Energy Change

Computation of the gain in secondary flow kinetic energy due to mixing is given by [5]

$$\Delta KE = \int_{\zeta}^{\xi} \rho v \left(\frac{v^2}{2} - \frac{v_e^2}{2}\right) d\xi \tag{25}$$

where ζ defines the jet boundary streamline illustrated in Fig.5 (the streamline is positioned so that the secondary mass flow through station i is equal to secondary mass flow through j). For the present discussion the dividing streamline position, b^*, is assumed known; Korst and Chow[5] discuss the typical approach of analysis. Expanding the equation for the change in kinetic energy yields

$$\Delta KE = Wb\rho\left[\int_{\zeta}^{1} (v^3 - vv_e^2) d\xi + \int_{1}^{\xi} (v^3 - vv_e^2) d\xi\right] \tag{26}$$

Substitution of the self-similar profiles into this expression and integrating the result provides

$$\Delta KE = Wb\rho[v_e^3(H_1 + H_5 - F_3 - F_4) + v_m v_e^2(H_3 - F_1) + v_m^2 v_e H_2 + v_m^3 H_4] \quad (27)$$

where the detailed expressions for the integrals H_i and F_i are given by Drummond[4]. What is important about the integrals is that they are *independent of time* and have closed form algebraic solutions; they also need only be computed once for a given shear boundary layer value.

Primary Flow Energy Change

Similar to the way in which the change in secondary flow kinetic energy was computed, the energy loss of the primary flow is given by

$$\Delta KE = \int_0^{\xi} \rho v \left(\frac{v^2}{2} - \frac{v_m^2}{2} \right) d\xi \quad (28)$$

where the limits of integration reflect interest in the domain of the primary jet cross-section. Completing the integral for station i yields

$$\Delta KE = Wb\rho[v_e^3 H_1 + v_e v_m^2 H_2 + v_m v_e^2 H_3 + v_m^3 H_4 - v_m^3 F_1 - v_e v_m^2 F_3] \quad (29)$$

Again, reference [4] provides the expressions for the integrals implied in F_i and H_i

DISCUSSION OF CASE STUDY

For complete verification of the proposed ejector modeling technique it is necessary to have available transient ejector performance data to compare with calibrated simulation output. At the present time, however, only steady-state tests have been conducted at NASA Lewis for the STOVL ejector shown in Fig.1 (see summary of Corsiglia et. al.[3]), but this is proposed to be adequate for ejector model calibration; by "calibration" it is meant that the unknown mixing parameter β and the kinetic energy constant C_1 have been computed for a given ejector configuration. In this regard a practical STOVL ejector test case to examine involves a step-function in the primary nozzle flowrate.

The first constant to compute is the mixing effectiveness parameter, β. Here, β is selected as the value that appears to provide reasonably accurate thrust predictions for all steady flow data points within a given performance window. Tests of the E7-D ejector (Fig.1) covering subsonic and choked primary flows suggested $\beta = 1.055$ provides the best general match between theory and experiment.

For a step-function change in the primary flow, the ejector, initially operating at a steady-state condition, asymptotically approaches a second steady-state condition. The desired C_1 value is the one which provides a match between the predicted asymptote and the known thrust at the second state. Figure 6 illustrates the situation for subsonic primary nozzle flow (within the performance window for β above) experiencing a change to 48.17 kg/s from 41.23 kg/s; the corresponding thrust levels are 212 N and 270 N, respectively. Thrust predictions for various C_1 values are shown in Fig. 6; the "best" asymptotic match appears to be for C_1 between 0.3 and 0.35.

The thrust predictions shown in Fig.6 appear to have a second-order response to the primary flow step-function. It seems the level of C_1 primarily influences the *level* of the thrust rather than shift the peak thrust overshoot. Under the second-order assumption the damping ratio is approximately 0.75 and the natural frequency of the ejector is on the order of 300 Hz.

CONCLUSION

A mathematical ejector model that includes system transients and has the potential to run in real time has been presented. The finite volume method permits time derivative of the mixing region field variables to be rapidly evaluated. Although final code verification awaits the availability of transient ejector data, ejector thrust predictions are intuitively reasonable. Future work must explore the proposed kinetic energy transfer function within a larger ejector performance window.

REFERENCES

1. Abramovich, G.N. (1963), *The Theory of Turbulent Jets*, MIT Press.
2. Addy, A.L. J.C.Dutton, and C.D.Mikkelsen (1981), "Ejector-diffuser theory and experiments," Report No. UILU-ENG-82-4001, Department of Mechanical and Industrial Engineering, University of Illinois at Urbana-Champaign.
3. Corsiglia, V., M.Dudley, B.Smith, and J.Farbridge (1989), "Large scale tests of an Ejector Augmentor STOVL," AIAA Paper 89-2905.
4. Drummond, C.K. (1988), "A control-volume method for analysis of unsteady thrust augmenting ejectors," NASA CR-182203.
5. Korst, H. and W.Chow (1966), "Non-isoenergetic turbulent jet mixing between two compressible streams at constant pressure," NASA CR-419.
6. Porter, J. and R.Squyers (1981), "A summary/overview of ejector augmentation theory and performance," USAF Technical Report No.R-91100-9CR-47.

NOMENCLATURE

A cross-sectional area
b jet half-width
B channel width
C_1 coefficient defined by equation(24)
KE kinetic energy
$\dot{m}$ mass flowrate
m_{cv} control volume mass
$\dot{M}$ momentum flux
M_{cv} control volume momentum
M_{1P} Mach number of primary nozzle flow
P pressure
t time
v velocity
x transverse coordinate
z streamwise coordinate
Z_i integral of defined function
β mixing effectiveness parameter
γ specific heat ratio
Λ normalized pressure profile
ρ density
Φ function defined by equation(4)
σ turbulent flow constant, equation(20)
ξ dimensionless transverse coordinate
ζ dimensionless jet streamline boundary

subscripts

cv control volume
e entrained stream
m primary stream centerline
$1s$ secondary steam at station 1
$1p$ primary stream at station 1

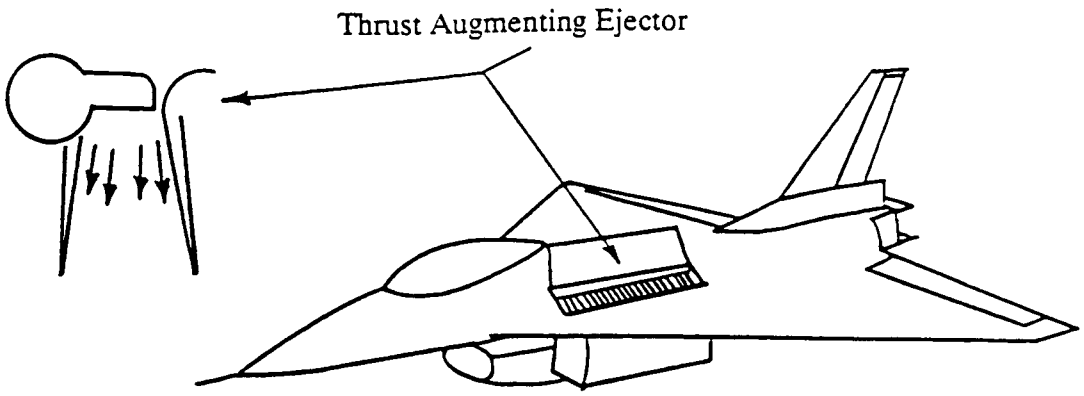

Fig. 1 E7/Ejector configured aircraft.

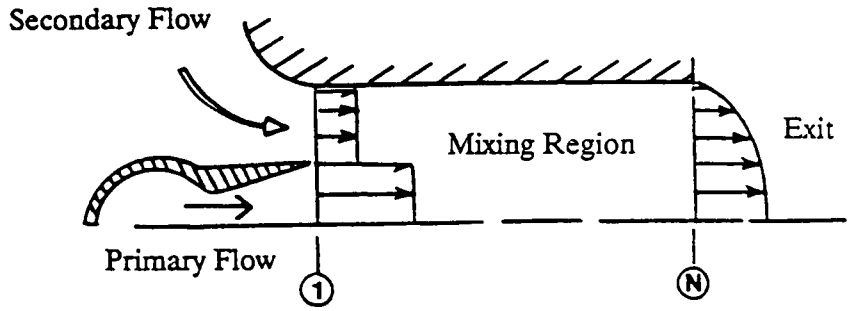

Fig. 2 Constant area mixing region.

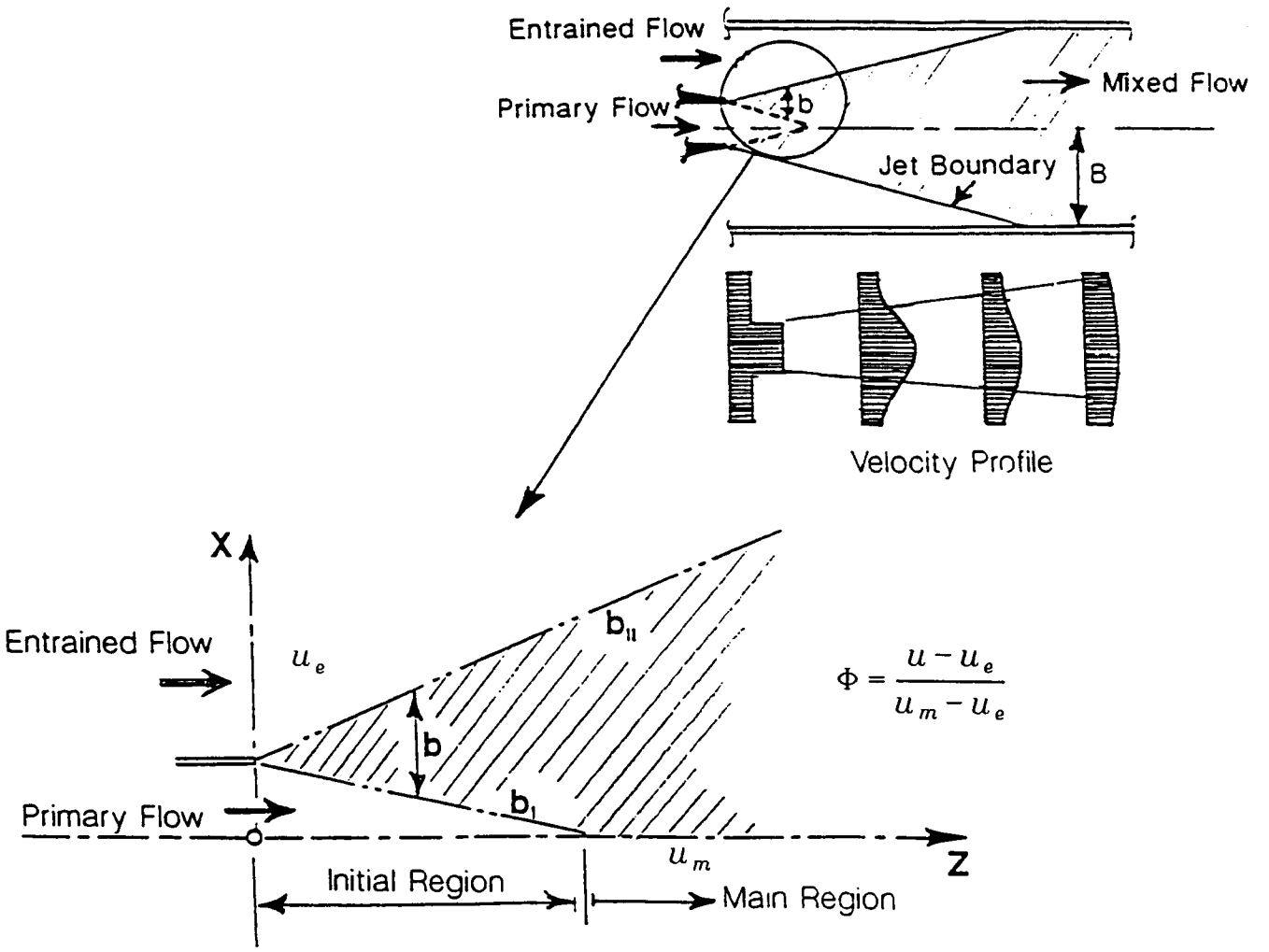

Fig. 3 Mixing region velocity profile.

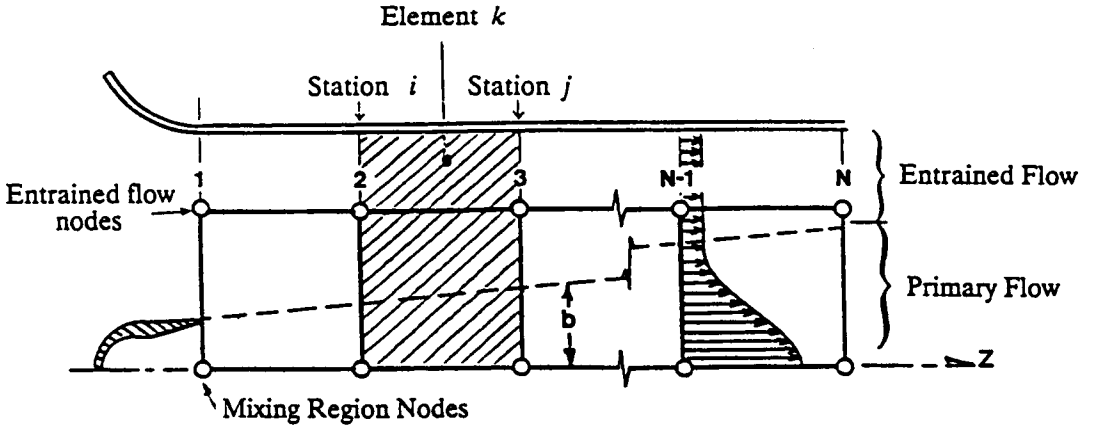

Fig. 4 Nomenclature for finite-volume

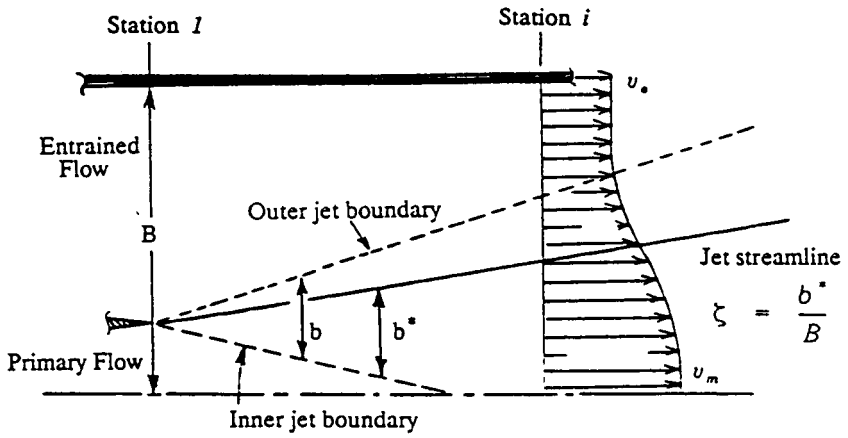

Fig. 5 Jet boundary streamline.

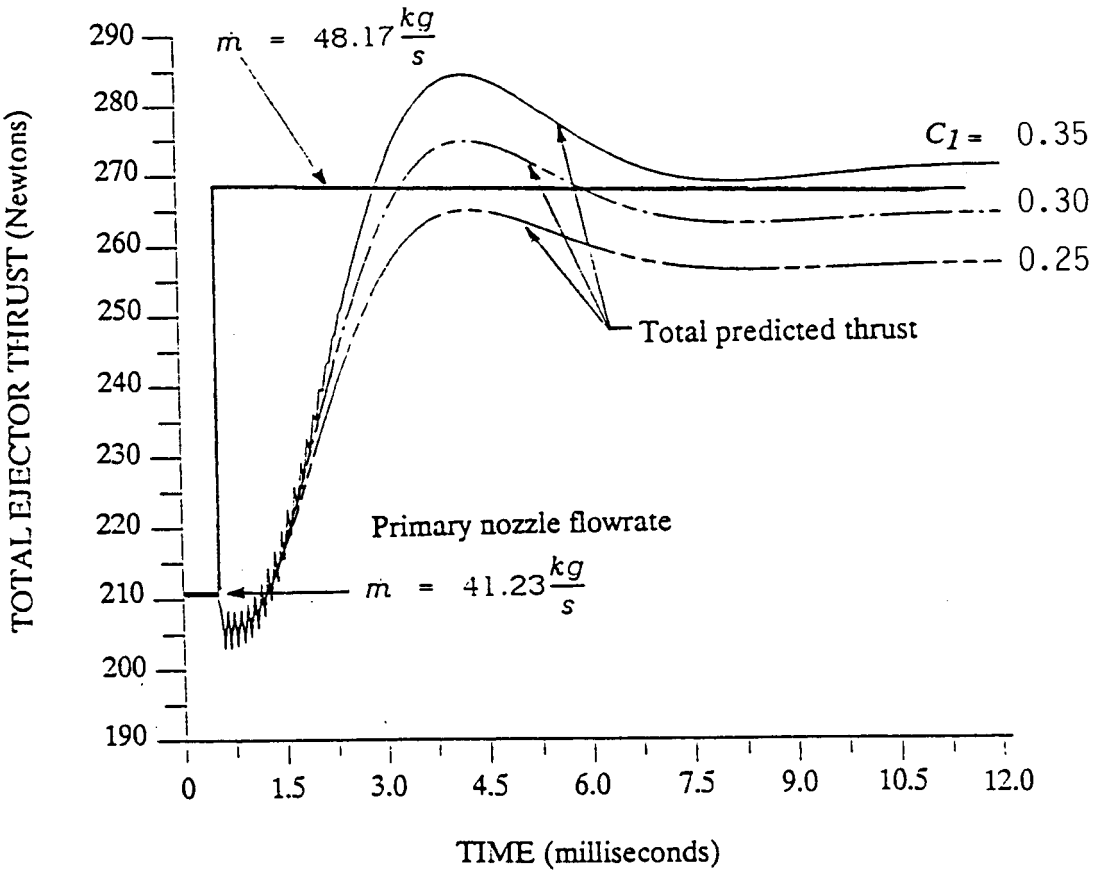

Fig. 6 Transient flow thrust prediction for various C_1 values.

NASA
National Aeronautics and Space Administration

Report Documentation Page

1. Report No.	2. Government Accession No.	3. Recipient's Catalog No.
NASA TM-102098		

4. Title and Subtitle	5. Report Date
A Model for Prediction of STOVL Ejector Dynamics	6. Performing Organization Code

7. Author(s)	8. Performing Organization Report No.
Colin K. Drummond	E-4861
	10. Work Unit No. 505-62-71

9. Performing Organization Name and Address	11. Contract or Grant No.
National Aeronautics and Space Administration Lewis Research Center Cleveland, Ohio 44135-3191	13. Type of Report and Period Covered Technical Memorandum

12. Sponsoring Agency Name and Address	14. Sponsoring Agency Code
National Aeronautics and Space Administration Washington, D.C. 20546-0001	

15. Supplementary Notes

Prepared for the Twentieth Annual Conference on Modeling and Simulation cosponsored by the University of Pittsburgh, IEEE, and ISA, Pittsburgh, Pennsylvania, May 4-5, 1989.

16. Abstract

A semi-empirical control-volume approach to ejector modeling for transient performance prediction is presented. This new approach is motivated by the need for a predictive real-time ejector sub-system simulation for STOVL integrated flight and propulsion controls design applications. Emphasis is placed on discussion of the approximate characterization of the mixing process central to thrust augmenting ejector operation. The proposed ejector model suggests transient flow predictions are possible with a model based on steady-flow data. A practical test case is presented to illustrate model calibration.

17. Key Words (Suggested by Author(s))	18. Distribution Statement
STOVL Simulation Ejectors Unsteady flow	Unclassified - Unlimited Subject Category 07

19. Security Classif. (of this report)	20. Security Classif. (of this page)	21. No of pages	22. Price*
Unclassified	Unclassified	14	A03

NASA FORM 1626 OCT 86

*For sale by the National Technical Information Service, Springfield, Virginia 22161